ARTICLE

# The transcription factor RelB restrains group 2 innate lymphoid cells and type 2 immune pathology in vivo

Lei Zhang[1,2], Yuanlin Ying[1], Shuqiu Chen[1,3], Preston R. Arnold[1], Fafa Tian[2], Laurie J. Minze, Xiang Xiao[1] and Xian C. Li[1,4]

The exact relationships between group 2 innate lymphoid cells (ILC2s) and Th2 cells in type 2 pathology, as well as the mechanisms that restrain the responses of these cells, remain poorly defined. Here we examined the roles of ILC2s and Th2 cells in type 2 lung pathology in vivo using germline and conditional *Relb*-deficient mice. We found that mice with germline deletion of *Relb* (*Relb*$^{-/-}$) spontaneously developed prominent type 2 pathology in the lung, which contrasted sharply with mice with T-cell-specific *Relb* deletion (*Relb*$^{f/f}$*Cd4-Cre*), which were healthy with no observed autoimmune pathology. We also found that in contrast to wild-type B6 mice, *Relb*-deficient mice showed markedly expanded ILC2s but not ILC1s or ILC3s. Moreover, adoptive transfer of naive CD4$^{+}$ T cells into *Rag1*$^{-/-}$*Relb*$^{-/-}$ hosts induced prominent type 2 lung pathology, which was inhibited by depletion of ILC2s. Mechanistically, we showed that *Relb* deletion led to enhanced expression of Bcl11b, a key transcription factor for ILC2s. We concluded that RelB plays a critical role in restraining ILC2s, primarily by suppressing Bcl11b activity, and consequently inhibits type 2 lung pathology in vivo.

**Key words:** Allergic inflammation; Innate lymphoid cells; NF-κB; RelB; Th2 cells; type 2 pathology

*Cellular & Molecular Immunology* (2021) 18:230–242; https://doi.org/10.1038/s41423-020-0404-0

## INTRODUCTION

Allergic lung inflammation, such as asthma, represents a classical example of Th2 immune activation and type 2 pathology, in which Th2 cells infiltrating the lungs produce high levels of the type 2 cytokines interleukin (IL)-4, IL-5, IL-9, and IL-13, which further perpetuate robust tissue inflammation and tissue damage.[1] These activities ultimately lead to the development of type 2 pathology in the lungs, which is characterized by airway hyperresponsiveness, goblet cell hyperplasia, mucin overproduction, eosinophilia, and extensive inflammatory cell infiltration.[2] Clearly, these findings provide strong evidence that Th2 cells are cytopathic effector cells in allergic inflammation. Interestingly, recent studies suggest that group 2 innate lymphoid cells (ILC2s), which express the same effector cytokine profile as Th2 cells, also play a role in the development of allergic lung inflammation.[3,4] However, the exact mechanisms that control ILC2s and their relationships to Th2 cells in producing type 2 pathology remain incompletely defined.

ILC2s belong to an emerging family of ILCs, which also includes ILC1s and ILC3s.[5] Interestingly, ILCs are highly enriched at barrier sites and mucosal surfaces (e.g., the skin, gut, and lungs), where they are closely involved in tissue repair and homeostasis, inflammatory responses, and defense against invading pathogens.[6] Developmentally, ILCs are derived from common lymphoid progenitors, which populate peripheral tissues during fetal and neonatal periods, with limited input from circulating progenitor cells in adulthood.[7] Functionally, ILC1s, ILC2s, and ILC3s have very different effector activities and can be distinguished from each other by differences in their secretion of effector cytokines and expression of distinct transcription factors.[8] Specifically, ILC1s express the transcription factor T-bet and produce the cytokines interferon (IFN)-γ and tumor necrosis factor-α, which are critical in cellular immunity, whereas ILC2s express GATA3 and readily produce the type 2 cytokines IL-4, IL-5, IL-9, and IL-13. However, ILC3s express the transcription factor RORγt and release the cytokines IL-17A and IL-22.[9] Thus, from a functional standpoint, ILC1s, ILC2s, and ILC3s closely mirror their adaptive counterpart Th1, Th2, and Th17 cells in the adaptive immune system.[10,11] Clearly, this raises interesting questions as to the exact relationships between these innate and adaptive cells in the initiation and outcomes of immune responses.

ILC2s are present in substantial numbers in the lungs[12] and, in contrast to T cells, they do not express somatically rearranged cell surface receptors that directly recognize foreign antigens, nor do they require a complex cellular differentiation process to acquire effector functions.[13] Instead, ILC2s are innate effector cells that are highly sensitive to the local milieu and are poised to rapidly release high levels of type 2 cytokines upon stimulation.[14] Because of this, ILC2s likely respond much earlier and faster than T cells during allergic lung inflammation. It remains unclear whether they directly cause tissue damage, but they clearly have the capacity to drive type 2 immune responses. In fact, studies in selected animal models seem to suggest a key role for ILC2s in type 2 immunity in the lungs.[3,15,16] What remains to be determined, however, is whether ILC2s are capable of producing type 2 pathology independent of Th2 cells and to what extent Th2 cells rely on ILC2s for their effector activities during type 2 responses and type

[1]Immunobiology and Transplant Science Center, and Department of Surgery, Houston Methodist Hospital, Texas Medical Center, Houston, Texas, USA; [2]Department of Neurology, Xiangya Hospital, Central South University, Changsha, China; [3]Department of Urology, Southeast University Zhongda Hospital, Nanjing, China and [4]Department of Surgery, Weill Cornell Medical College of Cornell University, New York, NY, USA
Correspondence: Xian C. Li (xcli@houstonmethodist.org)

Received: 9 December 2019 Accepted: 2 March 2020
Published online: 19 March 2020

2 pathology. These are significant issues and a clear understanding of them may have important clinical implications.

In the present study, we examined type 2 immunity in mice in which the nuclear factor-κB (NF-κB) family transcription factor RelB was genetically or conditionally deleted and found that RelB is a potent repressor of ILC2s, as its absence resulted in a marked expansion of ILC2s in vivo, which led to a strong Th2 response and type 2 lung pathology. We also generated *Rag1*$^{-/-}$*Relb*$^{-/-}$ double-knockout (DKO) mice, in which the ILC2s were also expanded. Moreover, adoptive transfer of naive *Relb*$^{-/-}$ CD4$^{+}$ T cells into *Rag1*$^{-/-}$*Relb*$^{-/-}$ hosts but not the *Rag1*$^{-/-}$ hosts readily induced type 2 immune pathology in the lungs, which was inhibited by depletion of ILC2s in the *Rag1*$^{-/-}$*Relb*$^{-/-}$ hosts. Mechanistically, we showed that RelB deletion led to enhanced expression of Bcl11b, a key transcription factor for ILC2s.[17] Thus, our data demonstrate that RelB is an intrinsic repressor of ILC2s, which are involved in the vigorous type 2 response and type 2 pathology in vivo.

## MATERIALS AND METHODS

### Animals

The following mice were purchased from The Jackson Laboratory (Bar Harbor, ME): C57BL/6 (#000664), *Relb*$^{-/-}$ (#002835), *Rag1*$^{-/-}$ (#002216), *Cd4-Cre* (#022071), congenic Thy1.1 (#000406), and *Stat6*$^{-/-}$ mice (#005977). *Rag2*$^{-/-}$*Il2rg*$^{-/-}$ DKO mice (#4111) were obtained from Taconic. *Irf4*$^{-/-}$ mice and *Relb4*$^{f/f}$ *Cd4-Cre* mice have been previously described.[18,19] To generate DKO mice, the *Relb*$^{-/-}$ mice were crossed with *Rag1*$^{-/-}$, *Irf4*$^{-/-}$, and *Stat6*$^{-/-}$ mice to generate *Rag1*$^{-/-}$*Relb*$^{-/-}$, *Relb*$^{-/-}$*Irf4*$^{-/-}$, and *Relb*$^{-/-}$*Stat6*$^{-/-}$ mice, respectively. In some experiments, germline *Relb*$^{-/-}$ mice were crossed with congenic Thy1.1 mice to generate Thy1.1 *Relb*$^{-/-}$ mice for ILC2 deletion and transfer purposes.

All mice used in these studies were confirmed by PCR-assisted genotyping or by flow cytometry to ensure the correct phenotype. Gender- and age-matched mice were used for individual experiments. All animals were maintained in a specific pathogen-free facility at the Houston Methodist Research Institute in Houston, Texas. Animal use and care were approved by the Houston Methodist Animal Care Committee in accordance with the Institutional Animal Care and Use Committee guidelines.

### Isolation of lymphoid cells from the spleen and tissues

Spleen cells were prepared by passing the spleen tissue through a 70 µm strainer. Lung tissues were minced and incubated for 30 min at 37 °C in Dulbecco's modified Eagle's medium (DMEM) containing 1 mg/ml collagenase type II, 1.5 mg/ml dispase II, and 50 µg/ml DNase I (all from Invitrogen). After digestion, lymphoid cells in the tissues were isolated in a 40% Percoll gradient by centrifugation for 10 min at 2300 r.p.m. Lymphoid cells in the liver were prepared by passing the tissues through 70 µm strainers, followed by 40% Percoll gradient centrifugation. Cells in the bone marrow (BM) were obtained by flushing the femurs and tibias with a syringe containing DMEM.

### Flow cytometry

The following antibodies were obtained from BioLegend: anti-CD3ε (145-2C11), CD4 (GK1.5), CD8 (53-6.7), CD44 (IM7), CD45 (30-F11), CD45.1 (A20), CD45.2 (104), CD62L (MEL-14), CD25 (PC61), NK1.1 (PK136), CD11c (N418), CD11b (M1/70), F4/80 (BM8), CD19 (6D5), Ly6G (1A8; 1:200), Gr-1 (RB6-8C5), TER-119 (TER-119), ST2 (DIH9), CD127 (A7R34), CD122 (TM-b1), Thy1.2 (53-2.1), CD135 (A2F10), CD117 (2B8), α4β7 (DATK32), Sca-1 (D7), T-bet (4B10), PE-donkey anti-rabbit IgG (Poly4064), IL-5 (TRFK5), and IL-4 (11B11). Anti-GATA3 (L50-823) and anti-PLZF (R17-809) were purchased from BD Biosciences. Anti-IL-13 (eBio13A), anti-RORγt (B2D), and anti-Thy1.1 (HISS1) were purchased from eBioscience. Anti-Bcl11b antibody (A300-384A) was purchased from Bethyl Laboratories.

For cell surface staining, single-cell suspensions were first stained with Zombie Aqua™ Viability Dye (Biolegend), followed by Fc blocking with anti-mouse CD16/32, and were then stained with the appropriate antibodies. Intracellular staining was performed as previously described,[19] using a Foxp3 staining buffer set for transcription factors (eBioscience) or a BD Cytofix/Cytoperm Plus kit (#554715) for cytokines. For cytokine staining, cells were first stimulated for 4 h with phorbol 12-myristate 13-acetate (50 ng/ml) and ionomycin (550 ng/ml; Sigma-Aldrich) in the presence of GolgiStop (BD PharMingen). For detection of apoptotic cells, cells were stained with an Annexin-V apoptosis detection kit (Biolegend, #640934) according to the manufacturer's recommendations. After staining, all samples were acquired using an LSRII and the data were analyzed with FlowJo v10 software.[20]

### Cell sorting and adoptive transfer

Single-cell suspensions were prepared from the lungs and were first stained with lineage markers (F4/80, CD11b, CD11c, Gr-1, TER1-119, and NK1.1), as well as CD45, CD90.2, and ST2. The ILC2s (CD45$^{+}$ Lin$^{-}$, CD90.2$^{+}$, ST2$^{+}$) were selectively gated and sorted with a FACSAria II cell sorter (BD Biosciences), with a sorting purity of >98%. To prepare thymic CD4 single-positive T cells, CD4$^{+}$ T cells from the thymus of 9-day-old *Relb*$^{-/-}$ mice (naive cells were identified as CD62L$^{+}$CD44$^{low}$) were first enriched from thymic cell suspension using a Dynabeads™ Untouched™ Mouse CD4 Cells Kit (Invitrogen, #11415D), followed by fluorescence-activated cell sorting (FACS) by gating on the CD4$^{+}$ CD8$^{-}$ fraction. For adoptive cell transfer, sorted ILC2s ($1 \times 10^5$/mouse) or thymic CD4 single-positive T cells ($1 \times 10^6$/mouse) were injected into recipient mice via tail vein injection.

### Deletion of ILC2s in vivo

Deletion of ILC2s in vivo was performed as previously reported.[21] Briefly, mice were treated with Thy1.2-specific mAbs (0.2 mg, clone 30H12; BioXcell) via intraperitoneal injection on days −2, 0, 5, 10, 15, 20, and 25, and day 0 was designated as the time of adoptive T-cell transfer. The deletion efficiency of ILC2s was confirmed by flow cytometry.

### Bone marrow reconstitution

BM cells were collected from the femurs and tibias of donor mice, and the mature T cells and B cells in the BM were removed with PE–anti-CD3 (2C11) and PE–anti-CD19 (6D5) antibodies, and anti-PE magnetic MicroBeads (Miltenyi Biotec). The remaining cells were used for reconstitution of the recipient mice, which were lethally irradiated (9 Gy) before BM reconstitution. Each recipient was then given $2 \times 10^7$ donor BM cells via the tail vein. The mice were kept under specific pathogen-free conditions and were used for analyses at 4–8 weeks after reconstitution.

### Tissue pathology and quantitative analyses

Mouse lungs were collected and fixed in fresh 10% neutral buffered formalin or 24–72 h. After fixation, the samples were placed in 70% ethanol at 4 °C and then processed at the Pathology & Histology Core at Baylor College of Medicine (Houston, TX) for further hematoxylin and eosin and periodic acid-schiff (PAS) staining. Semiquantitative analyses of peribronchiolar inflammation and airway goblet cell hyperplasia were performed in a double-blinded manner, as previously reported.[22]

Six randomly selected ×10 magnification fields were evaluated per mouse lung. Within each magnification field, five peribronchioles were randomly selected for inflammatory cell infiltration assessment (histological score) or PAS-positive cell scoring (PAS$^{+}$ score). Each airway was assigned a value for inflammatory cell infiltration as follows: 0 = normal; 1 = few cells; 2 = a ring of inflammatory cells one cell layer deep; 3 = a ring of inflammatory cells two to four cells deep; and 4 = a ring of inflammatory cells of >4 cells deep. Furthermore, PAS-stained sections were used to

analyze mucus production semiquantitatively. The scores for the abundance of goblet cells in each airway were determined by the ratio of PAS-positive cells to total epithelial cells as follows: 0: <5% goblet cells; 1: 5–25%; 2: 25–50%; 3: 50–75%; and 4: >75%. The five histological scores and $PAS^+$ scores from each magnification field were averaged to provide an overall histological score and $PAS^+$ score for each sample.

### Differentiation of naive $CD4^+$ T cells in vitro

Naive $CD4^+$ T cells ($CD62L^+CD44^{low}Foxp3GFP^-$) were FACS-sorted from the spleens of wild-type (WT) B6 and *Relb*$^{-/-}$ *Foxp3-gfp* reporter mice and stimulated with anti-CD3 (2 μg/ml, 2C11; eBioscience) in the presence of equal numbers of syngeneic antigen-presenting cells (APCs) in 96-well tissue-culture plates (Sigma-Aldrich) at $5 \times 10^4$ cells per well. APCs were prepared by depletion of T cells from total spleen cells with PE–anti-CD3 (2C11; Miltenyi Biotec) and anti-PE microbeads (Miltenyi Biotec), followed by a brief treatment with mitomycin C (50 μg/ml; Sigma-Aldrich) before each experiment. For induction of Th2 cells in vitro, the cells were activated in the presence of mouse IL-4 (10 ng/ml), mouse IL-2 (5 ng/ml), and anti-mouse IFN-γ (10 μg/ml). All recombinant cytokines were obtained from R&D Systems.

### Luciferase reporter assay

The luciferase reporter assay was performed as previously described.[23] Briefly, the −800 ~ +16 *Bcl11b* promoter region, containing the proximal 800 bp of the murine *Bcl11b* promoter and 16 bp after the transcription start site region, was cloned into the pGL4 luciferase reporter plasmid (Promega). 3T3 cells were transfected with the reporter constructs together with expression plasmids carrying cDNA encoding the full-length *Relb* or the transactivation domain (TAD)-deleted *Relb* or control plasmid using Lipofectamine 3000 (Invitrogen). After 36 h, the luciferase activities were analyzed using a dual-luciferase reporter assay system (Promega). Cotransfection with the *Renilla* luciferase expression vector was performed in all reporter assays. For all samples, the relative luciferase activity was calculated by dividing the firefly luciferase activity by the *Renilla* luciferase activity.

### Tracking ILC2s with EdU in vitro

FACS-sorted lung ILC2s (10,000 cells/well) from *Rag1*$^{-/-}$ and *Rag1*$^{-/-}$*Relb*$^{-/-}$ mice were cultured in 200 μl RPMI-1640 media containing 10% fetal bovine serum, penicillin and streptomycin, 2-mercaptoethanol, IL-2 (10 ng/mL), and IL-7 (10 ng/mL) at 37 °C for 3 days. The ILC2 proliferation status was assessed using the Click-iT EdU cell proliferation assay (Invitrogen). Briefly, the cells were pulsed with EdU in the tissue-culture plates for 2 h after 72 h of culture. The cells were prepared and assessed for EdU uptake according to the manufacturer's instructions.

### Statistical analyses

The Mann–Whitney test was used for analysis of histology and PAS scores. A two-tailed Student's *t*-test or one-way analysis of variance was used to generate *p*-values, as specified in the figure legends. *P*-values < 0.05 and <0.01 were considered statistically significant.

## RESULTS

### Germline deletion of *Relb* induced prominent type 2 pathology in the lungs

Compared with T cells in WT B6 mice, T cells in germline *Relb*-deleted mice (*Relb*$^{-/-}$ mice) showed a marked upregulation of CD44 and a reciprocal downregulation of CD62L expression on the cell surface; these cells also expressed the activation markers CD69 and Ki67 (Fig. 1a). These changes were consistent with an activated phenotype in vivo, as previously reported.[19,24] Moreover, a substantial number of *Relb*$^{-/-}$ $CD4^+$ T cells in the spleen, liver, and lungs spontaneously produced the Th2 cytokines IL-4, IL-5, and IL-13, which were primarily confined to activated $CD44^{high}$ T cells (Fig. 1b and Supplementary Fig. 1a). Further analysis of Th2-defining transcription factors showed that, in contrast to WT B6 $CD4^+$ T cells, *Relb*$^{-/-}$ T cells expressed high levels of GATA3, phosphorylated STAT6 (p-STAT6), and IRF4 (Fig. 1c), which are transcription factors that are strongly associated with Th2 cells.[1] To ascertain whether *Relb*$^{-/-}$ $CD4^+$ T cells acquired a Th2 program, we deleted *Irf4*, which showed the highest expression in *Relb*$^{-/-}$ $CD4^+$ T cells (Fig. 1c), from *Relb*$^{-/-}$ mice (i.e., *Relb*$^{-/-}$*Irf4*$^{-/-}$ DKO mice) and further examined the expression of Th2 cytokines by the *Relb*$^{-/-}$*Irf4*$^{-/-}$DKO T cells. As shown in Fig. 1d, $CD4^+$ T cells from DKO mice showed similar phenotypes as those from WT B6 mice; they did not express the Th2 cytokines IL-4 or IL-13, which was in stark contrast to that of *Relb*$^{-/-}$ $CD4^+$ T cells (Fig. 1d). We also deleted *Stat6* in *Relb*$^{-/-}$ mice and found that the *Relb*$^{-/-}$*Stat6*$^{-/-}$ DKO mice had a similar phenotype as that of *Relb*$^{-/-}$*Irf4*$^{-/-}$ DKO mice (Supplementary Fig. 1b). Assessments of tissue histology showed that in contrast to WT B6 mice, the *Relb*$^{-/-}$ mice developed prominent type 2 pathology in the lungs, which was characterized by extensive lymphocyte infiltration, primarily around the vasculature, and hyperplasia of mucin-producing cells in the airways (Fig. 1e, f). Interestingly, these changes were not observed in the lungs of *Relb*$^{-/-}$*Irf4*$^{-/-}$ DKO mice (Fig. 1e, f) or *Relb*$^{-/-}$*Stat6*$^{-/-}$ DKO mice (Supplementary Fig. 1c, d), which was consistent with the type 2 cytokine profiles shown in Fig. 1d and Supplementary Fig. 1b. Collectively, these data reinforce the notion that in *Relb*$^{-/-}$ mice, T cells are biased toward a Th2 phenotype to trigger type 2 lung inflammation.[24]

### *Relb*-deficient mice showed dramatically expanded ILC2s

As ILC2s are capable of expressing type 2 cytokines and the lungs host a large number of ILC2s,[3] we examined whether ILC2s are altered in *Relb*$^{-/-}$ mice and how they impact type 2 pathology in the lungs. Using the same gating strategies that are commonly used by others, as shown in Supplementary Fig. 2a, we compared the lung ILC2s from WT B6 and *Relb*$^{-/-}$ mice by flow cytometry. As shown in Fig. 2a and Supplementary Fig. 2b, c, we observed a marked expansion of ILC2s in the *Relb*$^{-/-}$ mice, as characterized by the strong expression of GATA3, ST2, and Sca-1 but not RORγt or T-bet (Fig. 2a). The absolute number of ILC2s expanded >10-fold in *Relb*$^{-/-}$ mice, whereas ILC3s and ILC1s did not show much change between WT B6 and *Relb*$^{-/-}$ mice (Fig. 2b). Importantly, the ILC2s in *Relb*$^{-/-}$ mice were functional and expressed high levels of the type 2 cytokines IL-4, IL-5, and IL-13 compared with those in the WT B6 controls (Fig. 2c, d). These findings clearly raised interesting questions about the exact roles and relationships between ILC2s and Th2 cells in type 2 pathology in *Relb*$^{-/-}$ mice.

We also examined the kinetics of Th2 induction, especially in relation to the in vivo expansion of ILC2s in *Relb*$^{-/-}$ mice. We found that $CD4^+$ T cells in 9-day-old *Relb*$^{-/-}$ mice did not express the Th2 cytokines IL-4, IL-5, and IL-13, nor did the mice show signs of type 2 lung pathology (Fig. 2e, f). However, such Th2 cytokines were strongly induced at later time points (Fig. 2e). Interestingly, the relative percentage and the absolute number of ILC2s in 9-day-old *Relb*$^{-/-}$ mice were already expanded dramatically when compared to those in age-matched WT B6 mice (Fig. 2g, h), suggesting that in the *Relb*$^{-/-}$ mice, activation of ILC2s may precede that of Th2 cells and that ILC2s and Th2 cells may be regulated by different mechanisms.

### T-cell-specific deletion of *Relb* failed to produce type 2 pathology

As a member of the NF-κB family, RelB is expressed by diverse cell types in addition to T cells.[25,26] In fact, in germline *Relb*-deleted mice, the development of medullary thymic epithelial cells (mTECs) is impaired, resulting in an expanded pool of autoreactive T cells in the periphery due to defective negative selection of

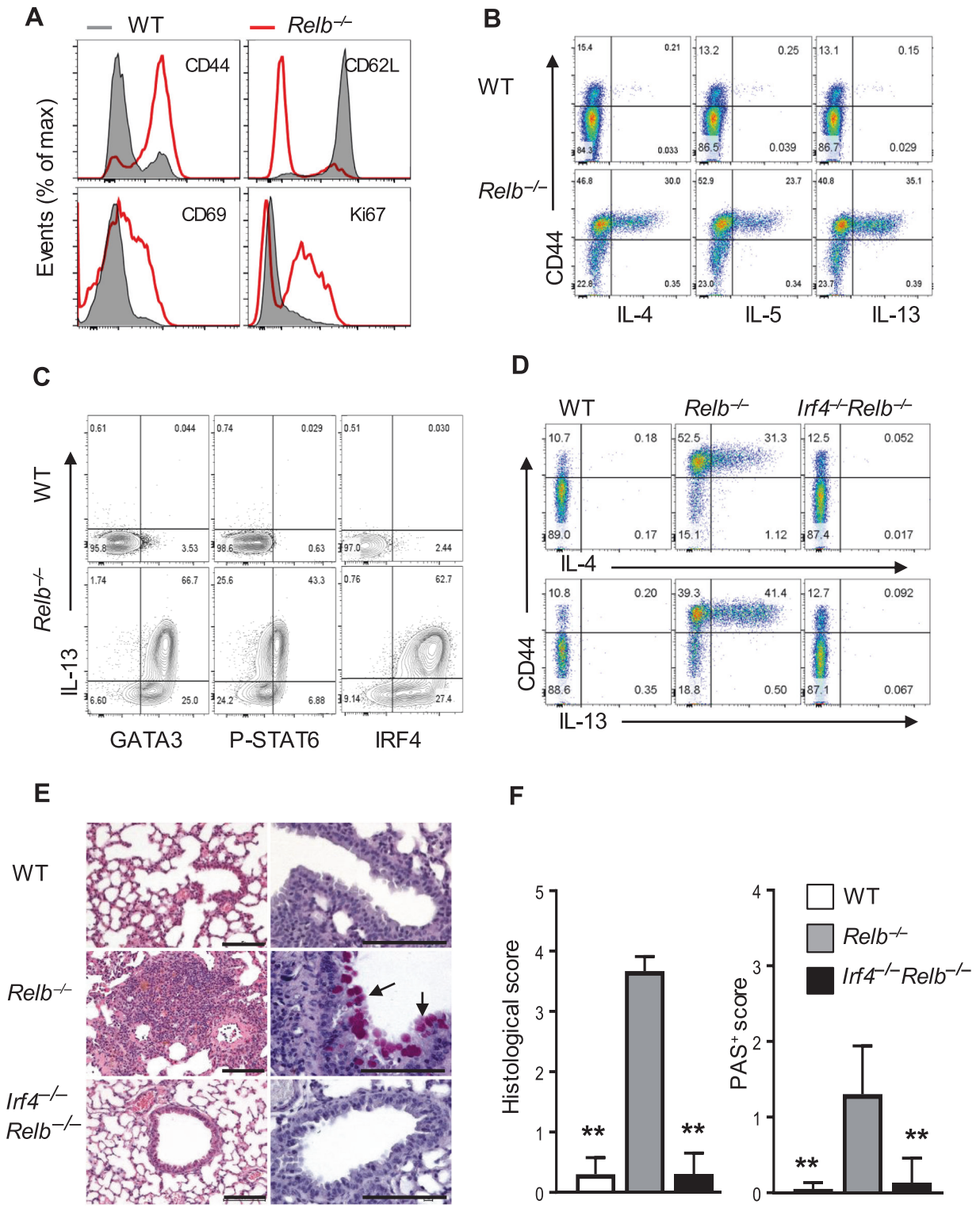


**Fig. 1** Development of type 2 pathology in germline *Relb* deleted mice. a Representative histograms showing the expression of CD44, CD62L, CD69, and Ki67 in splenic $CD4^+$ T cells from WT B6 and $Relb^{-/-}$ mice gated on $CD3^+CD4^+$ cells. **b**, **c** Flow cytometric analysis of intracellular expression of the Th2 cytokines IL-4, IL-5, and IL-13 (**b**) and the Th2-related transcription factors GATA3, p-STAT6, and IRF4 (**c**) in WT B6 and $Relb^{-/-}$ $CD4^+$ T cells. **d** Flow cytometric analysis of the intracellular cytokines IL-4 and IL-13 in WT B6, $Relb^{-/-}$, and $Relb^{-/-}Irf4^{-/-}$ DKO splenic $CD4^+$ T cells. **e** Representative images of H&E- (left) and PAS-stained (right) lung sections from WT B6, $Relb^{-/-}$, and $Relb^{-/-}Irf4^{-/-}$ DKO mice. **f** Histological and PAS scores of the mice shown in **e**. The data are representative of at least three independent experiments ($n = 5$ to 7) and are shown as the mean ± SD (**f**). Mann–Whitney test (**f**), $^{**}p < 0.01$. Numbers within flow plots indicate the percentage of gated cells. Scale bars represent 100 μm

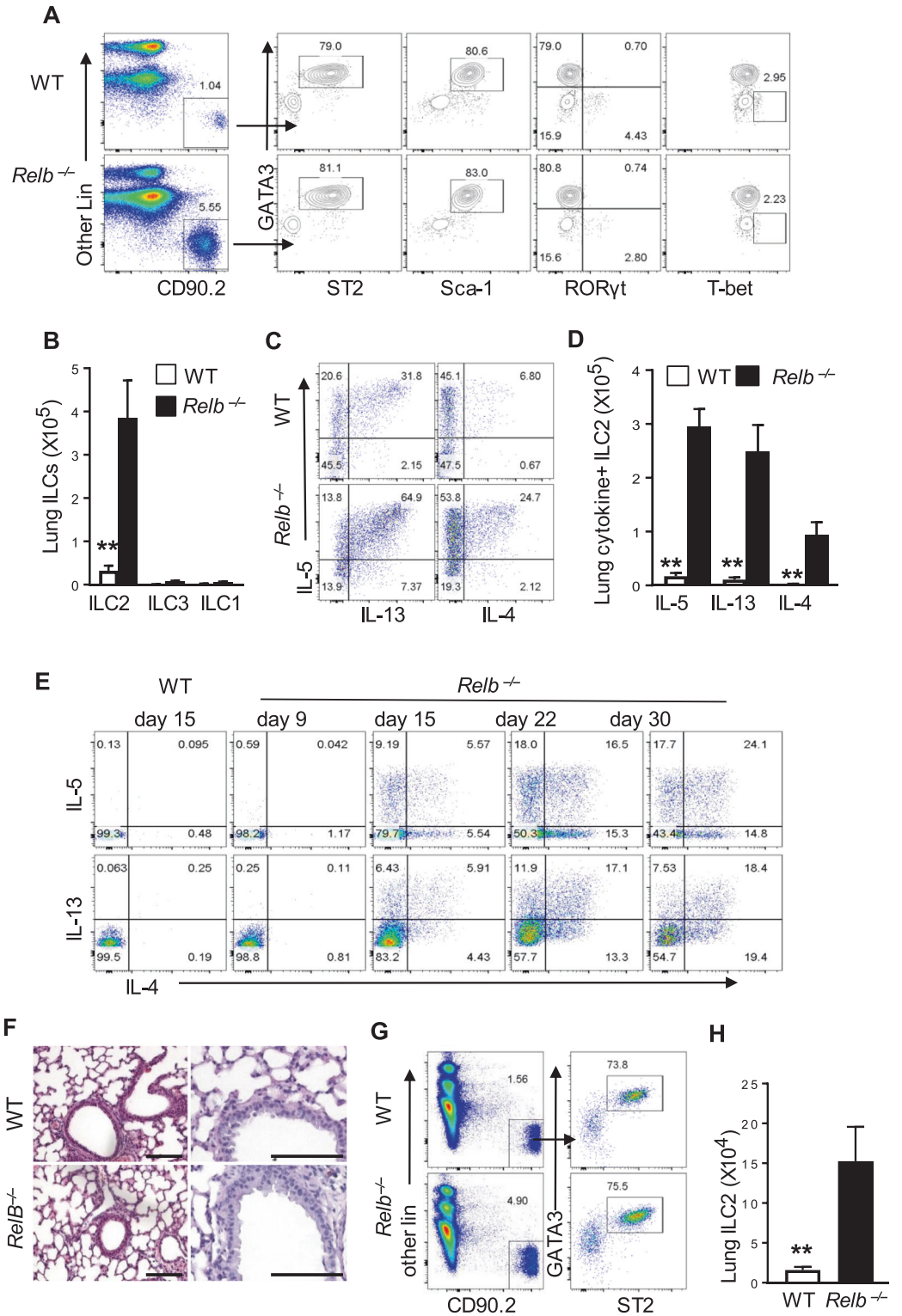


**Fig. 2** Analysis of ILC2s in WT B6 and germline *Relb*-deleted mice. **a** Flow cytometric analysis of ILC2s ($CD45^+$ $Lin^-$ $CD90.2^+$ $Gata3^+$ $ST2^+$), ILC1s ($CD45^+$ $Lin^-$ $CD90.2^+$ $Gata3^-$ T-$bet^+$) and ILC3s ($CD45^+$ $Lin^-$ $CD90.2^+$ $Gata3^-$ $ROR\gamma t^+$) in the lungs of WT B6 and $Relb^{-/-}$ mice gated on $CD45^+$ $CD3^-$ $NK1.1^-$ single live cells. **b** The absolute numbers of ILC1s, ILC2s, and ILC3s in lungs of WT B6 and $Relb^{-/-}$ mice were calculated. **c** Flow cytometric analysis of intracellular cytokines in lung ILC2s from WT B6 and $Relb^{-/-}$ mice. **d** The absolute numbers of IL-$5^+$, IL-$13^+$, and IL-$4^+$ lung ILC2s in WT B6 and $Relb^{-/-}$ mice. **e** Flow cytometric analysis of cytokine expression (IL-5, IL-13, and IL-4) in freshly prepared $CD4^+$ T cells from the spleens of WT B6 and $Relb^{-/-}$ mice at different times after birth as indicated in the figure. Representative images of H&E- (left) and PAS-stained (right) lung sections from 9-day-old WT B6 and $Relb^{-/-}$ mice. **g** Flow cytometric analysis of the relative frequency of ILC2s in the lungs of 9-day-old WT B6 and $Relb^{-/-}$ mice. **h** The absolute numbers of lung ILC2s from WT B6 and $Relb^{-/-}$ mice gated on $CD45^+$ $CD3^-$ $NK1.1^-$ single live cells. The data are representative of at least three independent experiments and are shown as the mean ± SD ($n = 5$ to 10). Two-tailed Student's *t*-test, $^{**}p < 0.01$. Numbers within flow plots indicate the percentage of gated cells and arrows from outlined areas on the left indicate gated cells that were subsequently analyzed

T cells in the thymus.[27] To address whether T-cell-specific RelB deletion is necessary and sufficient for type 2 pathology in vivo, we crossed *Relb*$^{f/f}$ mice with *Cd4-Cre* mice and generated *Relb*$^{f/f}$*Cd4-Cre* mice, in which *Relb* was selectively deleted in T cells (normal thymic mTECs and thymic selection). To our surprise, the *Relb*$^{f/f}$*Cd4-Cre* mice were completely healthy and did not show any signs of autoimmunity, which was in stark contrast to the *Relb*$^{-/-}$ mice. In fact, the *Relb*$^{f/f}$*Cd4-Cre* mice showed normal gross lung histology, with no obvious lymphocytic infiltrations, goblet cell hyperplasia, or mucus production (Figs. 3a and 2b). Analysis of freshly prepared T cells showed that while the *Relb*$^{-/-}$ CD4$^+$ T cells produced significant levels of the Th2 cytokines IL-4, IL-5, and IL-13, CD4$^+$ T cells from *Relb*$^{f/f}$*Cd4-Cre* mice failed to express these cytokines (Fig. 3c). To determine whether RelB-deficient T cells are inherently biased toward a Th2 program, we purified naive CD4$^+$ T cells from WT B6 and *Relb*$^{-/-}$ mice, cultured them in vitro for 4 days under Th2-polarizing conditions, and examined the induction of IL-4 and IL-13. As shown in Fig. 3d, e, the proportion of CD4$^+$ T cells that expressed the Th2 cytokines IL-4 and IL-13 was comparable between *Relb*$^{-/-}$ and WT B6 CD4$^+$ T cells, suggesting that the absence of RelB in T cells does not directly alter Th2 induction.

We also used the BM reconstitution approach in which BM cells were prepared from *Relb*$^{-/-}$ and WT B6 mice and injected into lethally irradiated syngeneic *Rag1*$^{-/-}$ hosts (i.e., mice with normal thymic epithelial cells). Eight weeks later, we analyzed the host mice for lung pathology and Th2 cytokine expression by reconstituted CD4$^+$ T cells. As shown in Fig. 3f, g, *Rag1*$^{-/-}$ hosts that were reconstituted with either WT B6 or *Relb*$^{-/-}$ BM failed to develop type 2 lung inflammation, which correlated with a lack of Th2 cytokine expression by the reconstituted CD4$^+$ T cells (Fig. 3h). Taken together, our results indicate that the strong Th2-biased immune responses observed in *Relb*$^{-/-}$ mice may also involve T-cell-extrinsic mechanisms.

T-cell-intrinsic vs. T-cell-extrinsic *Relb* deficiency in Th2 responses

The striking difference between *Relb*$^{-/-}$ and *Relb*$^{f/f}$*Cd4-Cre* mice prompted us to examine the T-cell-extrinsic mechanisms by which RelB impacts Th2 responses in vivo. We first bred *Rag1*$^{-/-}$*Relb*$^{-/-}$ DKO mice, in which RelB deficiency was confined to the innate compartment (i.e., non-T/B cells), and examined whether ILC2s were altered in *Rag1*$^{-/-}$*Relb*$^{-/-}$ mice. Compared with ILC2s in the *Rag1*$^{-/-}$ mice (in the lungs), those in the *Rag1*$^{-/-}$*Relb*$^{-/-}$ mice were increased substantially, either in the relative percentage (Fig. 4a) or in absolute cell numbers (Fig. 4b). Interestingly, the numbers of ILC1s and ILC3s were again comparable between the *Rag1*$^{-/-}$ and *Rag1*$^{-/-}$*Relb*$^{-/-}$ mice (Fig. 4b). Moreover, staining for type 2 cytokines showed that ILC2s in *Rag1*$^{-/-}$*Relb*$^{-/-}$ mice expressed much higher levels of type 2 cytokines IL-4, IL-5, and IL-13 than those in the *Rag1*$^{-/-}$ mice (Fig. 4c, d). We also created competitive BM chimeras, in which WT B6 and *Relb*-deficient BM cells were allowed to develop in the same irradiated *Rag2*$^{-/-}$*Il2rg*$^{-/-}$ hosts, and then compared the development of ILC2s in vivo 6 weeks later (also NK cells and T cells for comparison) (Fig. 4e). As shown in Fig. 4f, g, the generation of ILC2s from the *Relb*-deficient BM was selectively increased compared to those generated from the WT B6 BM, while the development of NK cells and T cells was comparable in irradiated hosts regardless of the use of *Relb*-deficient or *Relb*-sufficient BM cells. Taken together, these data suggest that RelB deficiency directly impacts the activities of ILC2s.

We also performed adoptive transfer experiments using *Rag1*$^{-/-}$ and *Rag1*$^{-/-}$*Relb*$^{-/-}$ mice as recipient mice. As shown in Fig. 5a, we isolated CD4$^+$ T cells from the thymus of 9-day-old WT B6 and *Relb*$^{-/-}$ mice (i.e., true naive T cells) and adoptively transferred them into *Rag1*$^{-/-}$ and *Rag1*$^{-/-}$*Relb*$^{-/-}$ hosts. The activity of the transferred CD4$^+$ T cells and changes in the host lungs were examined 4 weeks later. As shown in Fig. 5b, c, CD4$^+$ T cells from *Relb*$^{-/-}$ mice induced prominent lung pathologies in *Rag1*$^{-/-}$*Relb*$^{-/-}$ mice, as shown by cellular infiltration, goblet cell hyperplasia, and enhanced mucin production in the airways, while those transferred into the *Rag1*$^{-/-}$ hosts had little effect in the lungs (Fig. 5d). Interestingly, in both *Rag1*$^{-/-}$ and *Rag1*$^{-/-}$*Relb*$^{-/-}$ mice, adoptive transfer of WT B6 CD4$^+$ T cells did not induce obvious changes in the lungs (Fig. 5b, c, d). Furthermore, *Relb*$^{-/-}$ CD4$^+$ T cells in *Rag1*$^{-/-}$*Relb*$^{-/-}$ host mice produced substantial levels of the Th2 cytokines IL-4, IL-5, and IL-13, whereas those in *Rag1*$^{-/-}$ hosts failed to do so (Fig. 5e). Again, WT B6 CD4$^+$ T cells transferred to either the *Rag1*$^{-/-}$ or *Rag1*$^{-/-}$*Relb*$^{-/-}$ hosts failed to become Th2 cytokine-producing cells (Fig. 5e). These data suggest that for the resting CD4$^+$ T cells to trigger type 2 pathology in the time frame examined in the current study, the transferred T-cell population must contain a sufficient number of autoreactive cells (*Relb*$^{-/-}$ thymic CD4$^+$ T cells),[27–29] and that the host mice must have sufficient activated ILC2s (*Rag1*$^{-/-}$*Relb*$^{-/-}$ hosts).

To further examine the requirement of both *Rag1*$^{-/-}$*Relb*$^{-/-}$ hosts and naive *Relb*$^{-/-}$ thymic CD4$^+$ T cells in type 2 pathology, we again generated BM chimeric mice as shown in Fig. 5f. We reconstituted lethally irradiated *Rag1*$^{-/-}$ mice with congenic *Rag1*$^{-/-}$ or *Rag1*$^{-/-}$*Relb*$^{-/-}$ BM cells, and 6 weeks later, when optimal reconstitution occurred, we adoptively transferred naive *Relb*$^{-/-}$ thymic CD4$^+$ T cells into the reconstituted host mice. Four weeks later, we assessed the Th2 cytokine profiles and the lung pathology in the host mice. Once again, the transferred naive CD4$^+$ T cells acquired a Th2 phenotype and induced type 2 pathologies in *Rag1*$^{-/-}$*Relb*$^{-/-}$ BM reconstituted hosts but not in the *Rag1*$^{-/-}$ BM reconstituted mice (Fig. 5g, h, i). These data also suggest that cells in the *Rag1*$^{-/-}$*Relb*$^{-/-}$ deficient mice that support Th2 induction are hematopoietic in origin.

Role of *Relb*-deficient ILC2s in the induction of type 2 lung pathology

We took two different approaches to determine the role of ILC2s and their interactions with CD4$^+$ T cells in type 2 lung inflammation. The first approach involved adaptive transfer of *Relb*$^{-/-}$ thymic CD4$^+$ T cells into *Rag1*$^{-/-}$ hosts, followed by transfer of FACS-sorted ILC2s from *Rag1*$^{-/-}$*Relb*$^{-/-}$ DKO mice (5 doses in a 5-day interval). The host mice were sacrificed 28 days later for analyses (Supplementary Fig. 3a). As shown in Fig. 6a, b, *Rag1*$^{-/-}$ hosts that were adoptively transferred with the *Rag1*$^{-/-}$*Relb*$^{-/-}$ DKO ILC2s developed severe lung inflammation, with increased mucin-producing cells in the airways, compared to those of animals that were transferred with *Rag1*$^{-/-}$ ILC2s. Moreover, CD4$^+$ T cells that were transferred into *Rag1*$^{-/-}$ hosts with DKO ILC2s produced more Th2 cytokines than those with *Rag1*$^{-/-}$ ILC2s (Fig. 6c).

The other approach involved depletion of ILC2s in *Rag1*$^{-/-}$*Relb*$^{-/-}$ DKO mice. To this end, the *Rag1*$^{-/-}$*Relb*$^{-/-}$ hosts were given multiple doses of a depleting anti-Thy1.2 mAb, which targets the ILCs cells,[21] followed by adoptive transfer of *Relb*$^{-/-}$ thymic CD4$^+$ T cells (Thy1.1+), and analyses were performed 28 days later (Supplementary Fig. 3b). We first confirmed the depletion efficiency of the anti-Thy1.2 mAb in vivo (Supplementary Fig. 3c, d). Compared to inflammation in the control IgG-treated mice, depletion of ILC2s with anti-Thy1.2 markedly inhibited type 2 lung inflammation in *Rag1*$^{-/-}$*Relb*$^{-/-}$ hosts, as shown by tissue histology (Fig. 6d, e) and by the expression of Th2 cytokines (Fig. 6f). Taken together, these findings suggest that RelB deficiency in ILC2s promotes Th2 induction and, consequently, type 2 pathology in vivo.

RelB in the regulation of ILC2s and Bcl11b expression

To determine the mechanisms by which RelB controls ILC2s, we focused exclusively on the *Rag1*$^{-/-}$ and *Rag1*$^{-/-}$*Relb*$^{-/-}$ DKO models, as these models exclude the potential confounding effects of adaptive T cells on ILC2s in vivo. As shown in Fig. 7a, the

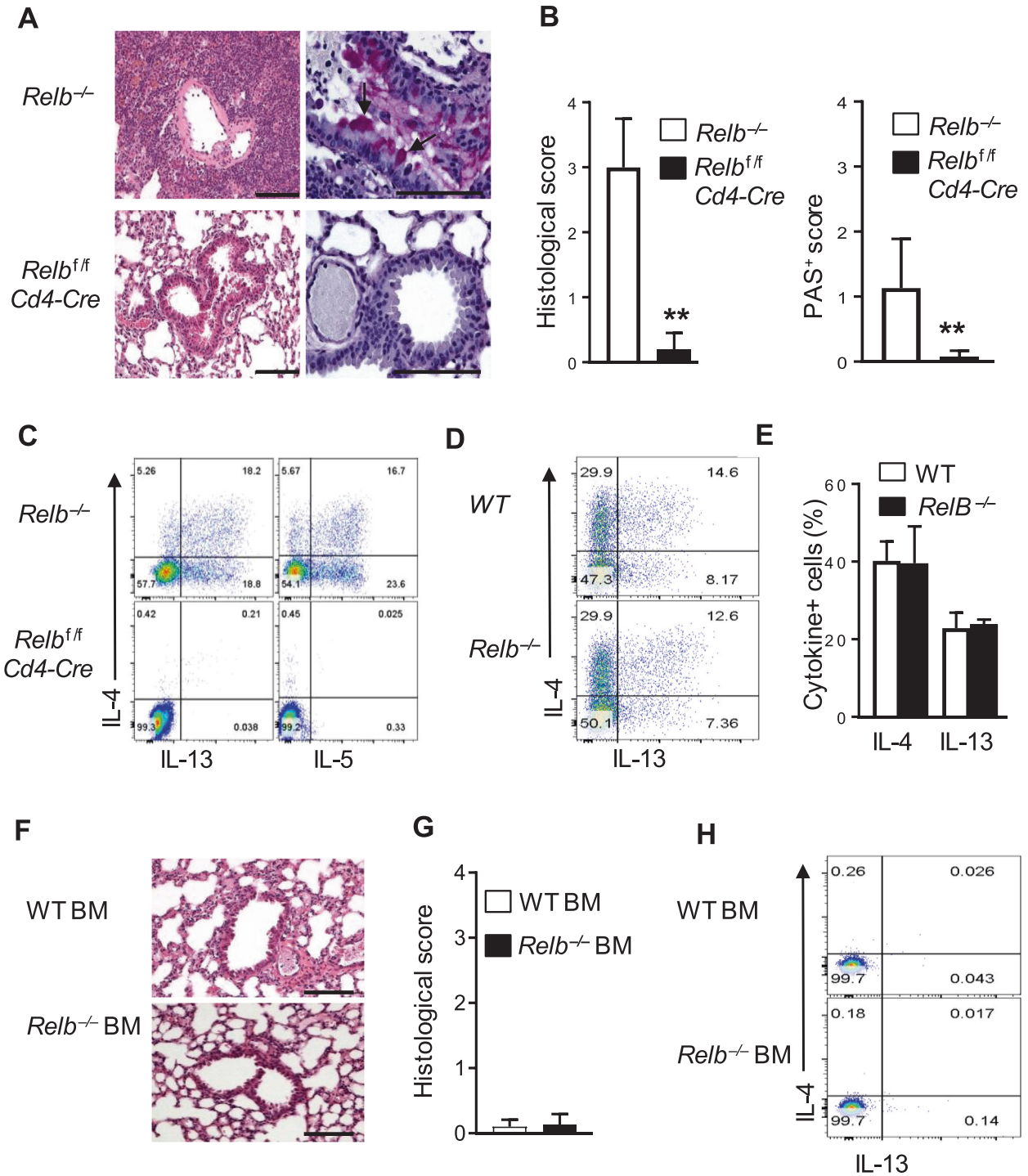


**Fig. 3** Tissue histology, T-cell phenotypes, and cytokine profiles in conditional *Relb*-deleted mice. **a** Representative images of H&E- (left) and PAS-stained (right) lung sections from $Relb^{-/-}$ and $Relb^{f/f}Cd4\text{-}Cre$ mice. **b** Histological and PAS scores of the mice shown in (**a**). **c** Flow cytometric analysis of the intracellular cytokines IL-4, IL-5, and IL-13 in splenic $CD4^+$ T cells from $Relb^{-/-}$ and $Relb^{f/f}Cd4\text{-}Cre$ mice. **d** Flow cytometric analysis of the intracellular cytokines IL-4 and IL-13 in WT B6 and $Relb^{-/-}$ $CD4^+$ naive T cells that were cultured in vitro under Th2 conditions for 4 days. **e** The percentage of IL-$4^+$ and IL-$13^+$ T cells are shown in **d**. **f**, **g** Representative images of H&E-stained lung sections (**f**) and related histological scores (**g**) from $Rag1^{-/-}$ recipient mice that were reconstituted with either WT B6 or $Relb^{-/-}$ BM at 8 weeks. **h** Flow cytometric analysis of the intracellular cytokines IL-4 and IL-13 in $CD4^+$ T cells from the host mice shown in (**f**). The data are representative of at least three independent experiments ($n = 5$ to 9) and are shown as the mean ± SD (**b**, **e**, **g**). The Mann–Whitney test was used for analysis in **b** and **g**, and two-tailed Student's *t*-test was used for analysis in **e**. $^{**}p < 0.01$. Numbers within flow plots indicate the relative percentage of gated cells. Scale bars represent 100 μm

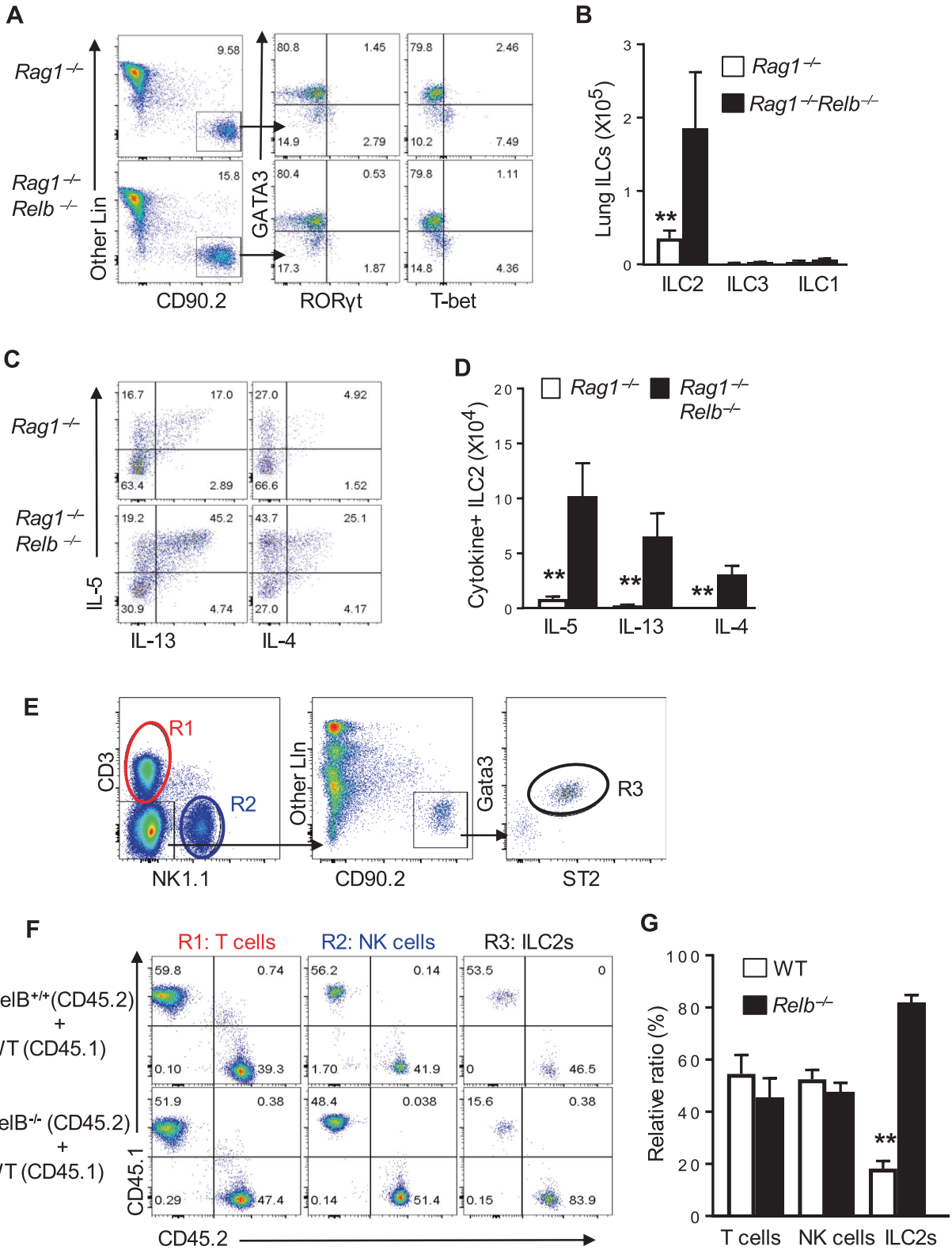


**Fig. 4** Analysis of ILC2s in *Rag1*$^{-/-}$ and *Rag1*$^{-/-}$*Relb*$^{-/-}$ double deficient mice, as well as in bone marrow chimeras. **a**, **b** Flow cytometry analysis of the relative frequencies (**a**) and the absolute cell numbers (**b**) of ILC1s, ILC2s, and ILC3s in the lungs of *Rag1*$^{-/-}$ and *Rag1*$^{-/-}$*Relb*$^{-/-}$ mice gated on CD45$^{+}$ NK1.1$^{-}$ single live cells. **c**, **d** Flow cytometric analysis of the relative frequencies (**c**) and the absolute numbers (**d**) of ILC2s from *Rag1*$^{-/-}$ and *Rag1*$^{-/-}$*Relb*$^{-/-}$ mice that expressed the cytokines IL-4, IL-5, and IL-13. **e** Gating strategy of various cell types in chimeric mice that were reconstituted with WT B6, *Relb*-deficient and *Reb*-sufficient BM cells 6 weeks later. R1 denotes T cells, while R2 and R3 denote NK cells and ILC2s, respectively. **f**, **g** The relative ratio of ILC2s, NK cells, and T cells in competitive chimeric mice that were reconstituted with *Relb*-sufficient and *Relb*-deficient BM cells. The data are representative of at least three independent experiments and are shown as the mean ± SD ($n = 5$). Two-tailed Student's *t*-test, $^{**}p < 0.01$. Numbers within flow plots indicate the percentage of gated cells and arrows from outlined areas on the left indicate gated cells that were analyzed

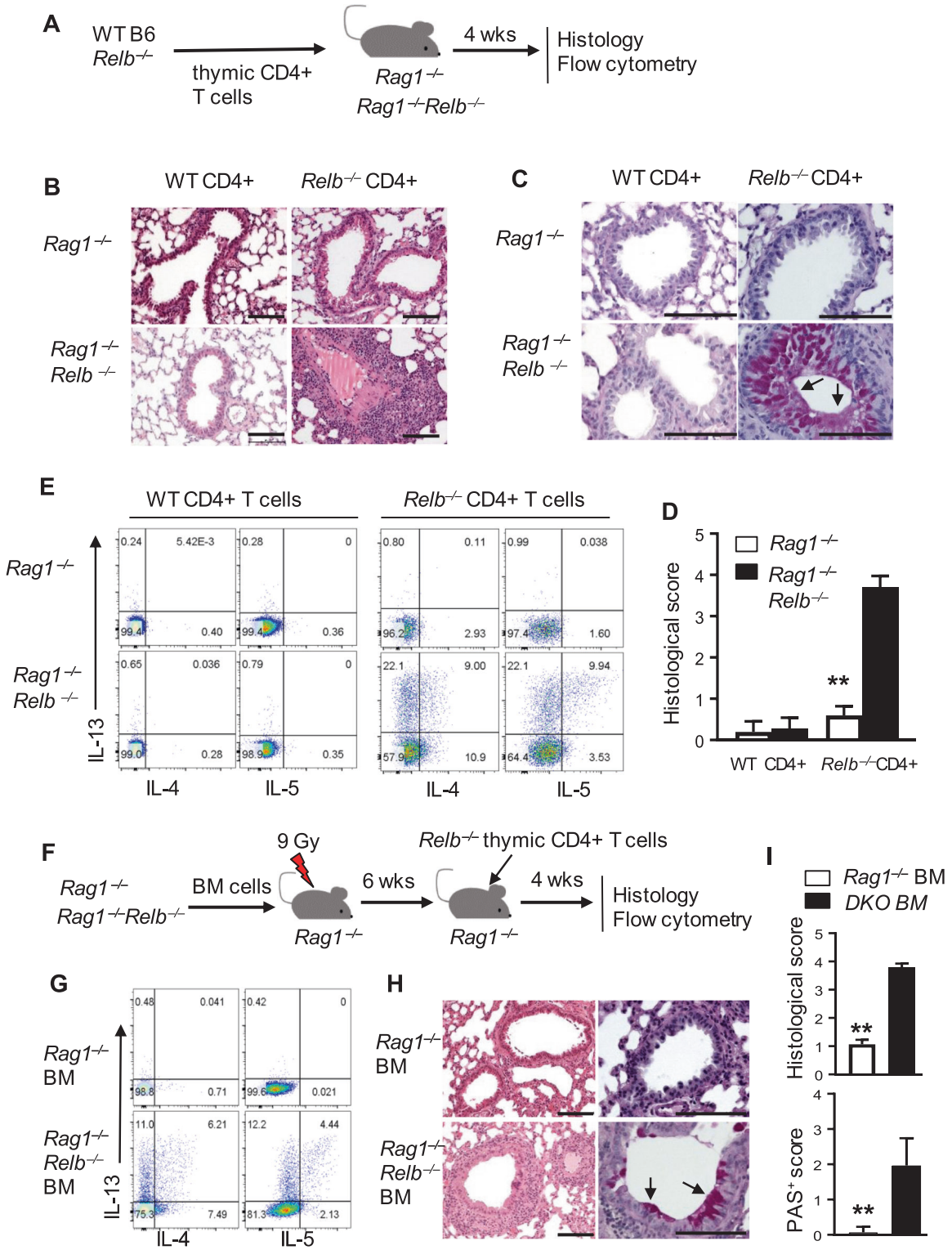


**Fig. 5** Impact of T-cell-intrinsic versus -extrinsic *Relb* deficiency on Th2 responses. **a** *Rag1*$^{-/-}$ or *Rag1*$^{-/-}$*Relb*$^{-/-}$ mice were intravenously injected with CD4$^{+}$ T cells from the thymus of 9-day-old WT B6 and *Relb*$^{-/-}$ mice and analyzed 4 weeks later by flow cytometry and histology. **b**, **c** Representative tissue images of H&E- (**b**) and PAS-stained (**c**) lung sections from *Rag1*$^{-/-}$ and *Rag1*$^{-/-}$*Relb*$^{-/-}$ recipients that were adoptively transferred with WT and *Relb*-deficient thymic CD4$^{+}$ T cells. **d** The histological score of the host mice shown in **b**. **e** Flow cytometric analysis of intracellular cytokines in transferred CD4$^{+}$ T cells recovered from *Rag1*$^{-/-}$ and *Rag1*$^{-/-}$*Relb*$^{-/-}$ recipients. The left panel shows WT CD4$^{+}$ T cells, and the right panel shows *Relb*$^{-/-}$ thymic CD4$^{+}$ T cells. **f** *Rag1*$^{-/-}$ or *Rag1*$^{-/-}$*Relb*$^{-/-}$ BM cells were intravenously transplanted into lethally irradiated (9 Gy) *Rag1*$^{-/-}$ recipients. Six weeks after BM reconstruction, the recipients were injected with *Relb*$^{-/-}$ thymic CD4$^{+}$ T cells and analyzed by flow cytometry and histology 4 weeks later. **g** Flow cytometric analysis of intracellular cytokines in transferred CD4$^{+}$ T cells from recipients that were injected with *Rag1*$^{-/-}$ BM or *Rag1*$^{-/-}$*Relb*$^{-/-}$BM cells. **h** Representative images of H&E- (left) and PAS-stained (right) lung sections from the mice shown in **g**. **i** Histological and PAS scores of the recipient mice shown in **h**. The data are representative of at least three independent experiments ($n = 5$) and are shown as the mean ± SD (**d**, **i**). $^{**}p < 0.01$. Numbers within flow plots indicate the percentage of gated cells. Arrows denote mucin-producing cells, and the scale bars represent 100 μm

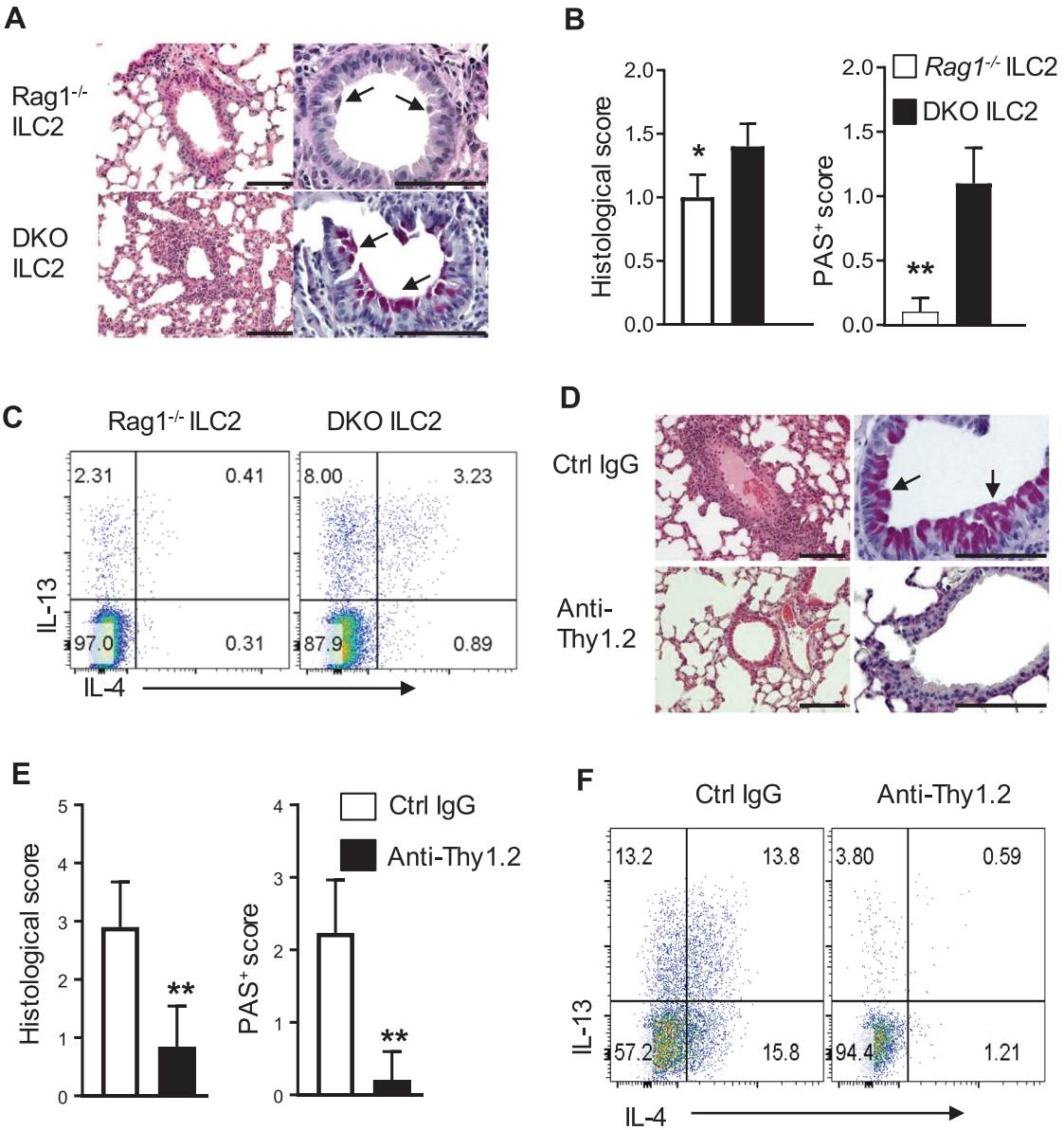


**Fig. 6** Role of ILC2s in the induction of type 2 pathology in vivo. **a** Representative images of H&E- (left) and PAS-stained (right) lung sections from host mice that were injected with *Rag1*$^{-/-}$ and *Rag1*$^{-/-}$*Relb*$^{-/-}$ ILC2s. **b** The histological and PAS scores of the mice shown in **a**. **c** Flow cytometric analysis of the intracellular cytokines IL-4 and IL-13 in CD4$^{+}$ T cells from the recipients shown in **a**. **d** Representative images of H&E- (left) and PAS-stained (right) lung sections from recipients with IgG control (without ILC2 deletion) or anti-Thy1.2 antibody (with ILC2 deletion). **e** Histological and PAS scores of the mice shown in **d**. **f** Flow cytometric analysis of the intracellular cytokines IL-4 and IL-13 in CD4$^{+}$ T cells from the recipients shown in **d**. The data are representative of two independent experiments ($n = 4$ to 6) and are shown as the mean ± SD (**b**, **e**). The Mann–Whitney test was used (**b**, **e**), $^{**}p < 0.01$. Numbers within flow plots indicate the percentage of gated cells. Arrows show mucin-producing cells, and scale bars represent 100 μm

proliferation of ILC2s in vitro was comparable in *Rag1*$^{-/-}$ and *Rag1*$^{-/-}$*Relb*$^{-/-}$ DKO mice, as assessed by EdU uptake assays. Moreover, the survival of ILC2s was also similar in the *Rag1*$^{-/-}$ and *Rag1*$^{-/-}$*Relb*$^{-/-}$ DKO mice as assessed by 7-ADD and Annexin-V staining (Fig. 7b), suggesting that the expansion of ILC2s in *Rag1*$^{-/-}$*RelB*$^{-/-}$ DKO mice is unlikely due to altered cell survival or proliferation.

We then examined ILC precursors in the BM by gating on the CD45$^{+}$ Lin$^{-}$CD127$^{+}$ population, and using a combination of cell surface markers,[30] we further partitioned the ILC precursors into distinct subsets, corresponding to the common lymphoid progenitors (CLP) and common helper-like lymphoid progenitors (CHILp), as well as precursors for ILC1s (ILC1p), ILC2s (ILC2p), and NK cells (NKp) (Fig. 7c), and then compared those subsets in *Rag1*$^{-/-}$ and *Rag1*$^{-/-}$*Relb*$^{-/-}$ DKO mice. We found a substantial increase in ILC2 precursor cells (ILC2ps) but not ILC1p, NKp, or CHILp in *Rag1*$^{-/-}$*Relb*$^{-/-}$ DKO mice (Fig. 7d), suggesting that RelB deletion selectively promotes the development of ILC2s. Analysis of specific transcription factors that are associated with ILC2s showed that Bcl11b expression was significantly upregulated in ILC2s in *Rag1*$^{-/-}$*Relb*$^{-/-}$ DKO mice compared with that in ILC2s in *Rag1*$^{-/-}$ mice (Fig. 7e, f), which was further confirmed by quantitative RT-PCR (Fig. 7g), while the expression of GATA3 and PLZF was comparable in ILC2s in *Rag1*$^{-/-}$ and *Rag1*$^{-/-}$*Relb*$^{-/-}$ DKO mice (Fig. 7h).

Bcl11b is critical in driving ILC2ps to differentiate into ILC2s.[31,32] Interestingly, analysis of the Bcl11b promoter region identified 4 putative κB binding sites (Supplementary Fig. 4), and in a

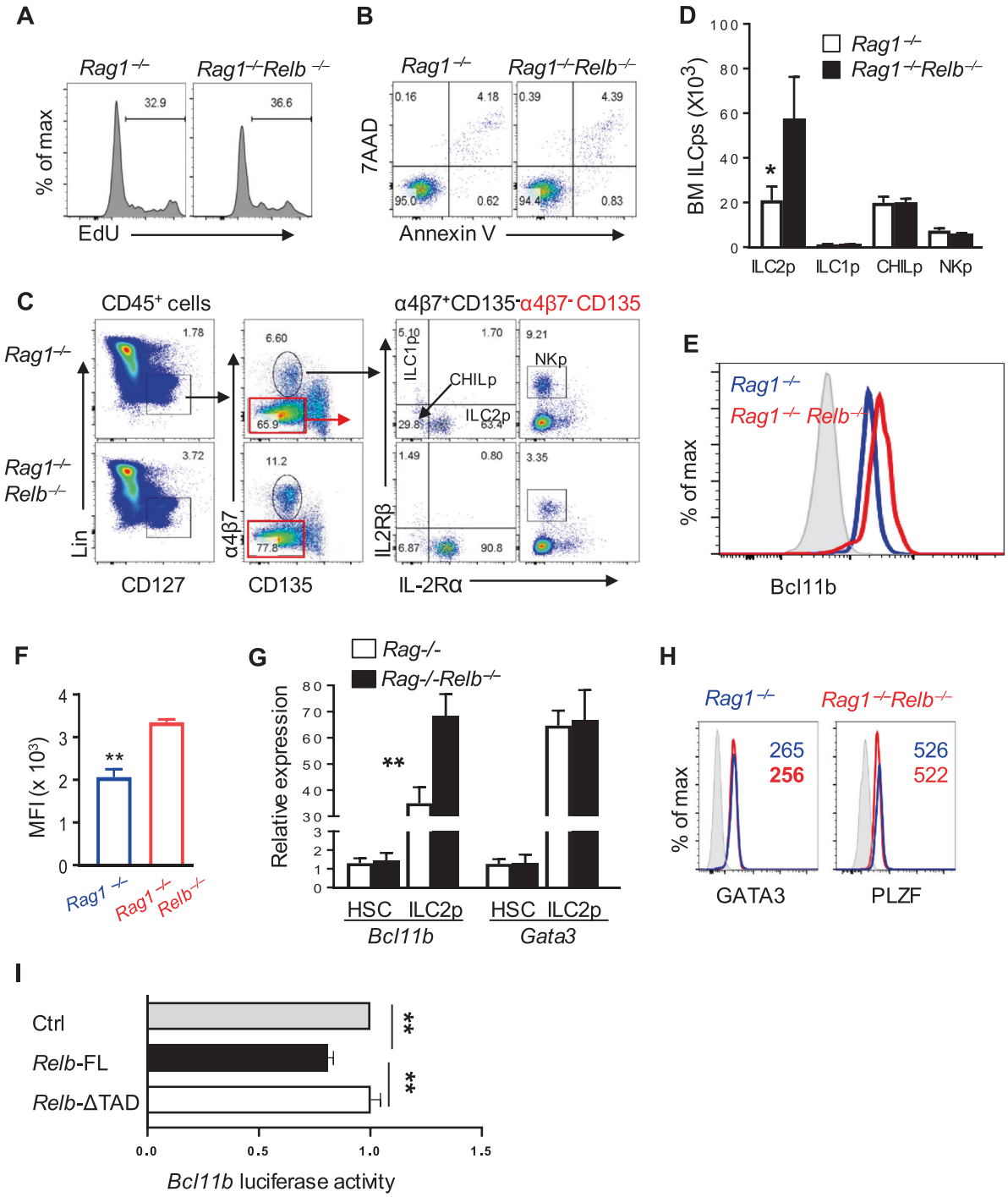


**Fig. 7** Roles of RelB in the regulation of ILC precursors, ILC2 survival, and transcription factor expression. **a**, Representative plots showing the EdU uptake of 3-day-cultured *Rag1*$^{-/-}$ and *Rag1*$^{-/-}$*Relb*$^{-/-}$ ILC2s. The numbers above the horizontal line are the frequencies of EdU-positive cells. **b**, Flow cytometry analysis of apoptotic cells in cultured ILC2s from *Rag1*$^{-/-}$ and *Rag1*$^{-/-}$*Relb*$^{-/-}$ mice by staining with Annexin-V and 7-AAD. **c**, Flow cytometric analysis of common progenitors to helper-like ILCs (CHILps: Lin$^-$ IL7R$^+$ CD135$^-$ Integrin α4β7$^+$ IL-2Rα$^-$ IL-2Rβ$^-$), ILC1ps (Lin$^-$ IL-7R$^+$ CD135$^-$ Integrin α4β7$^+$ IL-2Rα$^-$ IL2Rβ$^+$), ILC2ps (Lin$^-$ IL-7R$^+$ CD135$^-$ Integrin α4β7$^+$ IL-2Rα$^+$ IL-2Rβ$^-$) and NKps (Lin$^-$ IL-7R$^+$ CD135$^-$ Integrin α4β7$^-$ IL-2Rα$^-$ IL-2Rβ$^+$) from the bone marrow of *Rag1*$^{-/-}$ and *Rag1*$^{-/-}$*Relb*$^{-/-}$ mice. Arrows from outlined areas on the left indicate gated cells for subsequent analysis. **d** The absolute numbers of ILC2s, ILC1ps, CHILps, and NKps in the bone marrow of *Rag1*$^{-/-}$ and *Rag1*$^{-/-}$*Relb*$^{-/-}$ mice. **e** Representative plots showing the levels of Bcl11b expression in ILC2ps in the bone marrow of *Rag1*$^{-/-}$ and *Rag1*$^{-/-}$*Relb*$^{-/-}$ mice. The blue histogram represents *Rag1*$^{-/-}$ ILC2ps, and the red histogram represents *Rag1*$^{-/-}$*Relb*$^{-/-}$ ILC2ps. The gray histogram indicates isotype control staining. **f** The MFI of Bcl11b expression in ILC2s in the cells shown in **e** is summarized in bar graphs. **g** Quantitative RT-PCR showing the relative expression of Bcl11b and Gata3 transcripts in ILC2s and HSCs from *Rag1*$^{-/-}$ and *Rag1*$^{-/-}$*Relb*$^{-/-}$ mice. **h** Representative histograms of Gata3 and PLZF expression in ILC2s in *Rag1*$^{-/-}$ and *Rag1*$^{-/-}$*Relb*$^{-/-}$ mice (blue and red histograms, respectively). **i** Luciferase reporter assay showing Bcl11b promoter activity induced by control, *Relb*-FL, or *Relb*-ΔTAD constructs in 3T3 cells. The data are representative of at least three independent experiments ($n = 5$ to 12) and are shown as the mean ± SD (**d**, **g**, **i**). Student's *t*-test, $^{**}p < 0.01$. Numbers within flow plots indicate the relative percentage of gated cells

luciferase reporter assay, we showed that RelB expression significantly inhibited Bcl11b promoter activities (Fig. 7i). Deletion of the RelB TAD, which is required for RelB to engage target genes,[20] abolished the suppressive effect of RelB (Fig. 7i). These data suggest that RelB likely controls the development of ILC2s by repressing the transcription factor Bcl11b.

## DISCUSSION

In the present study, we made several interesting findings concerning the roles of RelB in type 2 immunity in vivo. Both ILC2s and Th2 cells are actively involved in driving type 2 lung pathology, which supports the current belief that both cell types conspire to produce robust type 2 responses.[33] We provide additional insights that each cell type plays a very different role during this process, depending on the timing, number of autoreactive T cells, and activation status of each cell type in vivo. Our data also suggest that in addition to direct pathogen challenges (e.g., dust mite and certain viruses) or direct airway epithelial injuries (e.g., papain) that usually trigger the release of alarmins (e.g., IL-25, IL-33, TSLP) to activate ILC2s to provoke type 2 pathology,[11] deletion of a single transcription factor, RelB, also recapitulates this process, which similarly involves ILC2s but occurs spontaneously without deliberate exogenous challenges. Importantly, the finding that RelB deficiency exhibits dramatic and selective effects on ILC2s but not ILC1s or ILC3s is novel and significant. This clearly places RelB on a growing list of transcription factors that control ILC2s and type 2 pathology in vivo, and a detailed understanding of this complex transcription network is undoubtedly an important and clinically relevant issue.[34]

As a member of the NF-κB family, RelB is expressed by multiple cell types in addition to immune cells; it constitutes an essential component in activation of the canonical and noncanonical NF-κB pathways.[35] As clearly highlighted by others,[26] this pathway has far-reaching implications in regulating many aspects of the immune and inflammatory responses. Germline *Relb* deletion clearly entails perturbations of diverse cell types, including both the immune and non-immune cell types that collectively give rise to type 2 lung pathology. This type of immune pathology develops spontaneously without initial epithelial damage involving external stimuli, as observed in other models.[36] Moreover, our studies using *Rag1*$^{-/-}$*Relb*$^{-/-}$ DKO mice as adoptive cell transfer hosts allowed us to provide substantial new insights in this regard. In the models we examined in the current study, it took at least two strikes to develop type 2 pathology in vivo in the absence of RelB: an expanded repertoire of autoreactive T cells, which develops due to a defect in mTECs and an expanded ILC2 pool in the recipient mice. It has been shown that mTECs express RelB, and conditional deletion of *Relb* in mTECs in *Relb*$^{f/f}$*K14*-Cre or *Relb*$^{f/f}$*Foxn1*-Cre mice impairs negative selection and results in the spontaneous development of autoimmunity.[27–29] We confirmed these findings and further showed that naive CD4$^{+}$ T cells (i.e., CD44$^{low}$CD62L$^{+}$) sorted from the thymus of 9-day-old *Relb*$^{-/-}$ thymus already contain sufficient autoreactive T cells that are capable of inducing type 2 pathology when transferred into immunodeficient *Rag1*$^{-/-}$*Relb*$^{-/-}$ hosts, which contain a substantial number of ILC2s (Fig. 2). Notably, RelB deficiency does not seem to directly affect mature T-cell activities, as T cells with conditional *Relb* deletion are not autoimmune, and their activation under Th2-polarizing conditions exhibits a cytokine profile similar to that of WT CD4$^{+}$ T cells (Fig. 3d). However, naive *Relb*$^{-/-}$ CD4$^{+}$ T cells fail to effectively induce type 2 lung pathology in the *Rag1*$^{-/-}$ mice, nor do WT B6 CD4$^{+}$ T cells in the *Rag1*$^{-/-}$*Relb*$^{-/-}$ hosts, even in the presence of substantial autoreactive T cells, suggesting that both components are required for the induction of type 2 pathology. This notion is further supported by our findings that depletion of ILC2s in *Rag1*$^{-/-}$*Relb*$^{-/-}$ mice prevented the induction of type 2 lung pathology and that *Relb*$^{-/-}$ thymic T cells had limited roles in type 2 responses in *Rag1*$^{-/-}$ mice. However, fully differentiated effector *Relb*$^{-/-}$ Th2 cells are capable of inducing type 2 pathologies in immunodeficient mice, even in the absence of ILCs (unpublished observations). Hence, despite a similar cytokine profile, ILC2s and Th2 cells have very different roles in the type 2 responses.

In addition to its role in other cell types,[19,37] the selective impact of RelB on ILC2s but not other types of ILCs is novel and highly interesting. The selective expansion of ILC2s in *Relb*-deficient mice is striking, especially in germline *Relb*-deleted mice (Fig. 2), which supports the notion that effector T cells also promote ILC2s in vivo, as they express certain cytokine receptors (e.g., IL-2Rα, IL-25R, IL-33R, and IL-7Rα) and therefore respond to such cytokines.[38] However, the expanded ILC2s in the immunodeficient *Rag1*$^{-/-}$*Relb*$^{-/-}$ mice were also substantial, with no apparent impacts on ILC1s or ILC3s, suggesting a direct role of RelB in regulating ILC2s. It is well known that ILCs (i.e., ILC1s, ILC2s, and ILC3s) are derived from common lymphoid progenitors (CLPs), which give rise to common helper-like lymphoid progenitors (CHILps) and ILC precursors (ILCps).[39] ILCps further differentiate into precursor cells for ILC1s, ILC2s, and ILC3s, which give rise to mature ILC subsets.[40] Each step is tightly regulated by a complex network of transcription factors, which are not fully understood.[5] Interestingly, recent studies using cell fate-mapping approaches showed that the commitment to ILC2 precursors (ILC2ps) and subsequently to mature ILC2s critically depends on the dynamic actions of the transcription factors TCF1, GATA3, RORα, Gfi1, and Bcl11b, of which Bcl11b in particular is highly expressed at the late stage of ILC2ps and specifically controls their transition into mature ILC2s.[40] Thus, deletion of Bcl11b selectively abrogates ILC2s in vivo, and mice reconstituted with either Bcl11b$^{-/-}$ fetal liver cells or Bcl11b$^{-/-}$ BM cells show a complete lack of ILC2s, whereas other subsets of ILCs are not affected.[17] Other studies suggest that Bcl11b is required for the expression of the ST2 chain of IL-33R, as well as GATA3 and Gfi1, which are critical in maintaining ILC2 identity.[40] In the present study, we provided evidence that Bcl11b is a preferential target of RelB, and by repressing its expression, RelB most effectively controls ILC2s in vivo. RelB deficiency led to expanded ILC2ps, which exhibited increased Bcl11b expression (Fig. 7). Moreover, the promoter region of Bcl11b contains multiple κB sites, and in a luciferase reporter assay, RelB expression consistently suppressed Bcl11b promoter activities, which was dependent on the TAD of RelB (Fig. 7), thus highlighting RelB as a potent checkpoint regulator of ILC2s.

Our study also raises several interesting questions that warrant further investigation in future studies. It remains to be determined why RelB selectively impacts ILC2s, especially when considering the diversity of ILCs and their progenitor cells, as well as the complexity of the transcription factors involved.[41] What induces or sustains RelB in ILC2s is also not clear and deserves further attention. Furthermore, in addition to an increase in cell numbers, *Relb*$^{-/-}$ ILC2s are functionally hyperactive, especially regarding IL-4 expression, and whether RelB regulates other aspects of ILC2s, in addition to repressing Bcl11b, also requires further clarification. In addition, RelB regulates dendritic cells, and its absence in dendritic cells also promotes airway inflammation.[37] The exact role of dendritic cells in lung pathology in our models warrants further investigation in future studies. Nevertheless, the identification of RelB as a critical checkpoint regulator of ILC2s, and consequently the type 2 pathology, is significant and may have important clinical implications.

## ACKNOWLEDGEMENTS

We acknowledge the Flow Cytometry Core and the Pathology Core at Houston Methodist for excellent services. This work was supported in part by the National Institutes of Health (R01AI080779) and the Kleberg Foundation.

## ADDITIONAL INFORMATION

The online version of this article (https://doi.org/10.1038/s41423-020-0404-0) contains supplementary material.

**Competing interests:** The authors declare no competing interests.

## REFERENCES

1. Nakayama, T. et al. Th2 cells in health and disease. *Annu. Rev. Immunol.* **35**, 53–84 (2017).
2. Muehling, L. M., Lawrence, M. G. & Woodfolk, J. A. Pathogenic CD4(+) T cells in patients with asthma. *J. Allergy Clin. Immunol.* **140**, 1523–1540 (2017).
3. Halim, T. Y. et al. Group 2 innate lymphoid cells are critical for the initiation of adaptive T helper 2 cell-mediated allergic lung inflammation. *Immunity* **40**, 425–435 (2014).
4. Winkler, C. et al. Activation of group 2 innate lymphoid cells after allergen challenge in asthmatic patients. *J. Allergy Clin. Immunol.* **144**, 61–69 (2019). e67.
5. Zook, E. C. & Kee, B. L. Development of innate lymphoid cells. *Nat. Immunol.* **17**, 775–782 (2016).
6. Panda, S. K. & Colonna, M. Innate lymphoid cells in mucosal immunity. *Front Immunol.* **10**, 861 (2019).
7. Schneider, C. et al. Tissue-resident group 2 innate lymphoid cells differentiate by layered ontogeny and in situ perinatal priming. *Immunity* **50**, 1425–1438 (2019). e1425.
8. Vivier, E., van de Pavert, S. A., Cooper, M. D. & Belz, G. T. The evolution of innate lymphoid cells. *Nat. Immunol.* **17**, 790–794 (2016).
9. Deckers, J., Branco Madeira, F. & Hammad, H. Innate immune cells in asthma. *Trends Immunol.* **34**, 540–547 (2013).
10. Vivier, E. et al. Innate lymphoid cells: 10 years on. *Cell* **174**, 1054–1066 (2018).
11. Kubo, M. Innate and adaptive type 2 immunity in lung allergic inflammation. *Immunol. Rev.* **278**, 162–172 (2017).
12. Germain, R. N. & Huang, Y. ILC2s - resident lymphocytes pre-adapted to a specific tissue or migratory effectors that adapt to where they move? *Curr. Opin. Immunol.* **56**, 76–81 (2019).
13. Drake, L. Y. & Kita, H. Group 2 innate lymphoid cells in the lung. *Adv. Immunol.* **124**, 1–16 (2014).
14. Lanier, L. L. Shades of grey–the blurring view of innate and adaptive immunity. *Nat. Rev. Immunol.* **13**, 73–74 (2013).
15. Gurram, R. K. & Zhu, J. Orchestration between ILC2s and Th2 cells in shaping type 2 immune responses. *Cell Mol. Immunol.* **16**, 225–235 (2019).
16. Zhu, J. T helper 2 (Th2) cell differentiation, type 2 innate lymphoid cell (ILC2) development and regulation of interleukin-4 (IL-4) and IL-13 production. *Cytokine* **75**, 14–24 (2015).
17. Califano, D. et al. Transcription factor Bcl11b controls identity and function of mature type 2 innate lymphoid cells. *Immunity* **43**, 354–368 (2015).
18. Wu, J. et al. Ablation of transcription factor IRF4 promotes transplant acceptance by driving allogenic CD4(+) T cell dysfunction. *Immunity* **47**, 1114–1128 (2017). e1116.
19. Li, J. et al. Role of the NF-kappaB family member RelB in regulation of Foxp3(+) regulatory T cells in vivo. *J. Immunol.* **200**, 1325–1334 (2018).
20. Xiao, X. et al. The costimulatory receptor OX40 inhibits interleukin-17 expression through activation of repressive chromatin remodeling pathways. *Immunity* **44**, 1271–1283 (2016).
21. McHedlidze, T. et al. Interleukin-33-dependent innate lymphoid cells mediate hepatic fibrosis. *Immunity* **39**, 357–371 (2013).
22. Ma, Y. et al. Sustained suppression of IL-13 by a vaccine attenuates airway inflammation and remodeling in mice. *Am. J. Respir. Cell Mol. Biol.* **48**, 540–549 (2013).
23. Xiao, X. et al. OX40 signaling favors the induction of T(H)9 cells and airway inflammation. *Nat. Immunol.* **13**, 981–990 (2012).
24. Weih, F. et al. Both multiorgan inflammation and myeloid hyperplasia in RelB-deficient mice are T cell dependent. *J. Immunol.* **157**, 3974–3979 (1996).
25. Zhang, L., Xiao, X., Arnold, P. R. & Li, X. C. Transcriptional and epigenetic regulation of immune tolerance: roles of the NF-kappaB family members. *Cell Mol. Immunol.* **16**, 315–323 (2019).
26. Sun, S. C. The noncanonical NF-kappaB pathway. *Immunol. Rev.* **246**, 125–140 (2012).
27. Jin, C. & Zhu, M. RelB intrinsically regulates the development and function of medullary thymic epithelial cells. *Sci. China Life Sci.* **61**, 1039–1048 (2018).
28. Weih, F. et al. Multiorgan inflammation and hematopoietic abnormalities in mice with a targeted disruption of RelB, a member of the NF-kappa B/Rel family. *Cell* **80**, 331–340 (1995).
29. Riemann, M. et al. Central immune tolerance depends on crosstalk between the classical and alternative NF-kappaB pathways in medullary thymic epithelial cells. *J. Autoimmun.* **81**, 56–67 (2017).
30. Diefenbach, A., Colonna, M. & Koyasu, S. Development, differentiation, and diversity of innate lymphoid cells. *Immunity* **41**, 354–365 (2014).
31. Yu, Y. et al. The transcription factor Bcl11b is specifically expressed in group 2 innate lymphoid cells and is essential for their development. *J. Exp. Med.* **212**, 865–874 (2015).
32. Walker, J. A. et al. Bcl11b is essential for group 2 innate lymphoid cell development. *J. Exp. Med* **212**, 875–882 (2015).
33. Sonnenberg, G. F. & Hepworth, M. R. Functional interactions between innate lymphoid cells and adaptive immunity. *Nat. Rev. Immunol.* **19**, 599–613 (2019).
34. Serafini, N., Vosshenrich, C. A. & Di Santo, J. P. Transcriptional regulation of innate lymphoid cell fate. *Nat. Rev. Immunol.* **15**, 415–428 (2015).
35. Zhang, Q., Lenardo, M. J. & Baltimore, D. 30 Years of NF-kappaB: a blossoming of relevance to human pathobiology. *Cell* **168**, 37–57 (2017).
36. Martinez-Gonzalez, I., Steer, C. A. & Takei, F. Lung ILC2s link innate and adaptive responses in allergic inflammation. *Trends Immunol.* **36**, 189–195 (2015).
37. Nair, P. M. et al. RelB-deficient dendritic cells promote the development of spontaneous allergic airway inflammation. *Am. J. Respir. Cell Mol. Biol.* **58**, 352–365 (2018).
38. Roediger, B. et al. IL-2 is a critical regulator of group 2 innate lymphoid cell function during pulmonary inflammation. *J. Allergy Clin. Immunol.* **136**, 1653–1663 (2015). e1657.
39. Constantinides, M. G., McDonald, B. D., Verhoef, P. A. & Bendelac, A. A committed precursor to innate lymphoid cells. *Nature* **508**, 397–401 (2014).
40. Ishizuka, I. E., Constantinides, M. G., Gudjonson, H. & Bendelac, A. The innate lymphoid cell precursor. *Annu Rev. Immunol.* **34**, 299–316 (2016).
41. Walker, J. A. et al. Polychromic reporter mice reveal unappreciated innate lymphoid cell progenitor heterogeneity and elusive ILC3 progenitors in bone marrow. *Immunity* **51**, 104–118 (2019). e107.